Powder Technology 380 (2021) 567–573

Contents lists available at ScienceDirect

Powder Technology

journal homepage: www.elsevier.com/locate/powtec

Effect of strain rate on powder flow behaviour using ball indentation method

Umair Zafar [a], Colin Hare [a,b], Ali Hassanpour [a], Mojtaba Ghadiri [a,*]

[a] School of Chemical and Process Engineering, University of Leeds, Leeds LS2 9JT, UK
[b] Department of Chemical and Process Engineering, University of Surrey, Guildford, Surrey GU2 7XH, UK

ARTICLE INFO

Article history:
Received 18 October 2018
Received in revised form 5 November 2020
Accepted 23 November 2020
Available online 27 November 2020

Keywords:
Powder flowability
Ball indentation method
High shear strain rate
Cohesive powder flow
Flow resistance

ABSTRACT

There are a number of techniques available for characterising powder flow behaviour, most of which are carried out under quasi-static conditions. Quasi-static methods are commonly used to define the conditions for the flow initiation, but they are inadequate for characterising the shear strain rate sensitivity of powder flow. The number of devices available to capture powder behaviour under dynamic conditions is indeed very limited. The very few commercially available instruments all require a large sample, which is not desirable for early stages of product development. We have recently proposed the use of ball indentation for characterising flow resistance of cohesive powders. The technique can be applied at very low consolidation stress levels (much less than 1 kPa) and requires only a small sample quantity, typically a few mm^3. Previous work showed a good correlation of flowability with established methods under quasi-static conditions. Therefore, an attempt is made to extend the method to dynamic conditions and investigate the sensitivity of the stresses on the shear strain rate for a range of powders, including glass ballotini, α-lactose monohydrate, calcium carbonate (Durcal) and limestone. The results show the existence of a threshold boundary above which the flow resistance experienced by the penetrating ball becomes dependent on the shear strain rate. This is in line with the trends reported in the literature. Therefore, the ball indentation technique has the potential to be used to assess powder flowability at high strain rates.

1. Introduction

There is a great interest in understanding the rheometry of cohesive powders due to the dynamic nature of industrial processes operating in continuous mode. Many techniques exist for characterising powder flowability in the quasi-static regime. However, powders do not exhibit the same behaviour under quasi-static and dynamic flow conditions [11]. In the quasi-static regime, resistance to motion is brought about through frictional contacts between particles. As the strain rate is increased sliding friction at contacts become less influential as particle collisions become dominating. There have been a number of studies focusing on high strain rates, known as the rapid flow or collisional regime (Tirupataiah and Sundararajan, 1990; [12]). Extensive work has been reported in literature on development of constitutive models of flow in this regime for non-cohesive powders, based on the kinetic theory of gases [8,13,19]. Between the quasi-static and rapid regimes, there exists an intermediate flow regime as addressed by Tardos et al. [21]. This flow regime is actually more prevalent in process industry, but it is difficult to quantify, as the boundaries between the regimes may vary for different types of materials.

Savage et al. [20] and Tardos et al. [21] investigated the transition between the slow to rapid granular flow regimes. In order to characterise this transition, Tardos et al. [21] devised a Couette type device in which they analysed the shearing response of a powder sample between two co-axial vertical cylinders rotating at differential speeds and classified the flow regimes based on the dimensionless shear strain rate, γ^*, given by Eq. (1).

$$\gamma^* = \gamma\left(\frac{d_p}{g}\right)^{1/2} \tag{1}$$

where γ is the shear strain rate (defined by the characteristic speed divided by the shear zone depth), d_p is the particle size and g is the gravitational acceleration. The boundaries between flow regimes are graphically illustrated in Fig. 1, in which the quasi-static regime is delineated by the region dominated by friction and having a low dimensionless shear strain rate of the order of 0.2 or less. In the dynamic flow regime the frictional forces are small, as high speed collisions between particles become more significant at dimensionless shear strain rates greater than 0.3, where the shear stress increases with strain rate to

* Corresponding author.
E-mail address: M.Ghadiri@leeds.ac.uk (M. Ghadiri).

https://doi.org/10.1016/j.powtec.2020.11.057

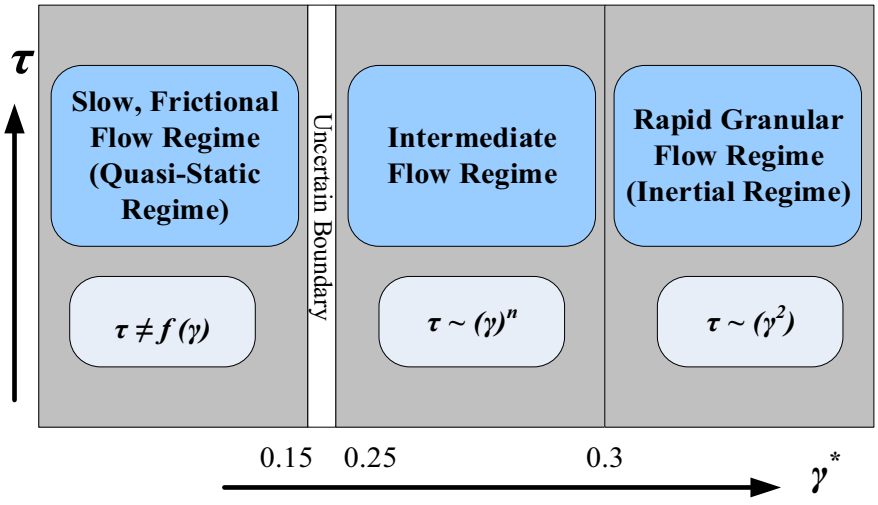

Fig. 1. Classification of flow regime according to Tardos et al. [21].

the power 2. In the middle of these two regimes there exists the intermediate flow regime, where the shear stress contributions of both collisional and frictional contacts between particles are comparable. The power index therefore is in the range of 0–2.

In contrast, Klausner et al. [10] showed increasing shear stress, τ, and stress ratio (τ/σ, where σ is normal stress) with strain rate in the frictional (quasi-static) regime. Within the intermediate regime the stresses increased with strain rate for silica, yet reduced for polymer particles. Behaviour similar to that of the silica particles has been observed in DEM simulations of cohesive glass beads in the FT4 Powder Rheometer by Hare and Ghadiri [5].

The flow regime boundaries found in DEM simulations of the Couette device by Vidyapati et al. (2012) were in agreement with the experimental measurements of Tardos et al. [21], showing that the shear stress is independent of the strain rate in the quasi-static regime. By increasing the strain rate, fluctuations in the shear stress start to increase and the dependency of shear stress on strain rate becomes prominent. Pasha et al. [18] observed similar increasing fluctuations at high strain rates in DEM simulations of dynamic ball indentation. The DEM simulations of Vidyapati et al. (2012) also showed that for monodisperse non-cohesive spheres the transition between regimes and the power law relationship are not sensitive to particle properties and operational details.

An alternative dimensionless number to represent the flow regimes of powders is the inertial number, I, given by Eq. (2).

$$I = \gamma d_p \sqrt{\rho_p / P} \tag{2}$$

where ρ_p is the particle density and P is the pressure.

MiDi [15] considered powder flow in six different configurations, including plane shear, chute flow and a rotating drum. The evolution of stresses with strain rate was found to follow similar trends to those reported by Tardos et al. [21]. As noted by Nan et al. [17] the dimensionless shear strain rate given by Eq. (1) is a simplified version of Eq. (2), when pressure P is equal to $\rho_p dg$. So Eq. (2) characterises the full span of flow regime more generally, where $I < 10^{-3}$ for quasi-static flow, $10^{-3} < I < 10^{-1}$ for dense inertial flow and $I > 10^{-1}$ for collisional flow. It should also be noted that in the development of constitutive equations, non-local rheology must be considered, and it is insufficient to consider only a single geometry [3,14]. Moreover, Mort et al. [16] urge caution for relating theory developed in simple systems to more complex flows.

More recently there have been attempts to develop flow prediction models spanning the three regimes. Chialvo et al. [2] developed a model of bulk friction as a function of the inertial number, based on molecular dynamic simulations of non-cohesive, frictional soft spheres. Berger et al. [1] analysed the scaling behaviour of cohesive granular flows and proposed a method for incorporating the effect of bulk cohesion in the inertial number for describing the dynamic flow resistance due to shearing. Nan et al. [17] analysed the particle flow behaviour by DEM simulations in the presence of air drag in the FT4 Powder Rheometer. They report that the increase in bulk friction with the inertial number could be expressed by a linear relationship, having an intercept at low shear strain rates corresponding to the quasi-static conditions. Jenkins and Berzi [9] compared predictions from the simple kinetic theory with those from the deformation theory to describe the dense inertial flow regime. Their work on simple homogenous shear flows showed good agreement, though it has not yet been applied to more complex flows.

The preceeding discussion demonstrates that powders exihibit diverse dynamic flow behaviour influenced by wide ranging constitutent particles properties. Despite considerable development in the analyses and modelling as recently reviewed by Ghadiri et al. [4], the prediction of cohesive powder flow still remains a grand challenge. Therefore, experimental characterisation of powder flow behaviour is a necessary first step. For instances where the quantity of powder available for testing is very small, for example less than 1 g, the only practical way to assess powder flowability is by the Ball Indentation Method (BIM), as first proposed by Hassanpour and Ghadiri [6] and later analysed by Pasha et al. (2013) and Zafar et al. [24]. Under such conditions the currently available commerical instruments are unsuitable. However, development of this method has been limited to quasi-static range of shear strain rates, with the exception of Tirapelle et al. [22], who used the same approach as presented here and evaluated the dynamic hardness of two types of titanium dioxide, corn starch flour and α-lactose monohydrate crystals. They demonstrated that flow resistance typically increased in the intermediate regime. Furthermore, they showed that the achievable shear strain rate range could be extended by manipulating indenter size and density, and provided a generalised relationship to determine optimum operating conditions for the test. In the present work we explore the sensitivity of flow resistance to strain rate for four different powders, i.e. fine cohesive glass ballotini, inhalation-grade of α-lactose monohydrate, which is much finer than that used by Tirapelle et al. [22], limestone (BCR) and calcium carbonate (Durcal). High strain rates are achieved by dropping a glass ball onto a powder

bed at various velocities and the impact process is recorded by a high speed video camera in order to determine the impact depth and strain rate.

2. Materials and methods

In this work, cohesive glass ballotini with a sieve cut of 45–63 μm were used as a model material. They were made cohesive by a silanisation process, applying a commercially available silane coating, having a functional group of heptane, known as Sigmacote®, supplied by Sigma-Aldrich®. The procedure reported by Zafar et al. (2014) for silanisation, drying time and temperature was followed. Cohesive glass ballotini were used as they are spherical and suitable for numerical simulation by Discrete Element Method, carried out in another piece of work which ran parallel with this work [18]. Other materials used in this work were two commercial calcium carbonate powders, i.e. Durcal 15, BCR limestone and α-lactose monohydrate powder used in the pharmaceutical industry with the commercial name Lactohale 300, supplied by DMV International, the Netherlands. Lactohale 300 is used for dry powder inhalation and its flowability under small loads and using a very small quantity is the subject of great interest. Durcal 15 and limestone powders are fine and cohesive and often used for calibration purposes and widely available. Scanning electron micrographs of the test materials are shown Fig. 2. The particle size distributions of the test materials were measured by Malvern Mastersizer 2000 using the wet dispersion method. The glass ballotini were dispersed in deionized water, whilst propan-2-ol was used as the carrier medium for the other materials. For particle size measurements, three repeats of each material were carried out, each at 10 s time intervals with 30 s duration. The characteristics particle sizes d_{10}, d_{50} and d_{90} of the particle size distribution on the volumetric basis are given in Table 1. For flowability characterisation in the quasi-static regime, the Schulze Ring Shear (RST-XS) tester was used. A family of yield loci were obtained for all the material samples and the unconfined yield strength was determined a function of the major principal stress. The results are shown for all the test materials in Fig. 3. The ratio of the major principal stress over the unconfined yield strength is commonly known as the flow function coefficient, which is an indicator of powder flowability under different stress states. The range of flow function coefficients for the test materials is shown in Table 2. All the experiments reported in this study were carried out at the temperature range of 20-23 °C and 38–45% relative humidity.

Table 1
Characteristic measures d_{10}, d_{50} and d_{90} of the particle size distributions obtained by the wet dispersion method (volume basis).

Material	d_{10} (μm)	d_{50} (μm)	d_{90} (μm)
Glass ballotini (45–63)	35	55	87
Durcal 15	2	15	30
Limestone	5	7	24
Lactohale 300	3	5	9

It can be seen from Figs. 2 and 3 that the four test materials have different particle size, shape, and surface morphologies. Lactohale 300 (milled grade of α-lactose monohydrate) is the finest of all the test materials and hence is the most cohesive. The flow classification for Durcal 15, silanised glass ballotini and limestone is similar over the range of pre-shear normal stresses used.

Ball indentation measurements at low strain rates were carried out using the Instron 5566 mechanical testing machine (Instron Corp., USA). Sample filling was done using the sieving method of Zafar et al., (2017), to achieve a uniform packing of the powder bed in the die and then pre-consolidated by a stainless steel piston using a 10 N load cell which had a resolution of 1 mN. The flow resistance is characterised by the hardness of the bed, as measured by indentation with a spherical

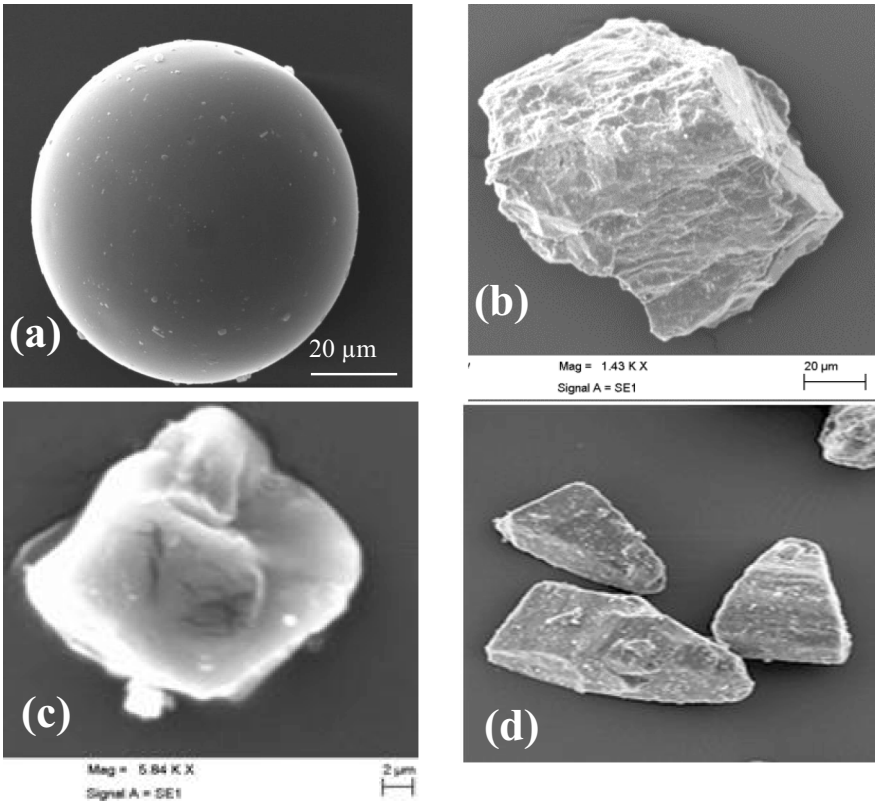

Fig. 2. Sample material: (a) silanised glass ballotini; (b) Durcal 15; (c) BCR limestone; and (d) Lactohale 300.

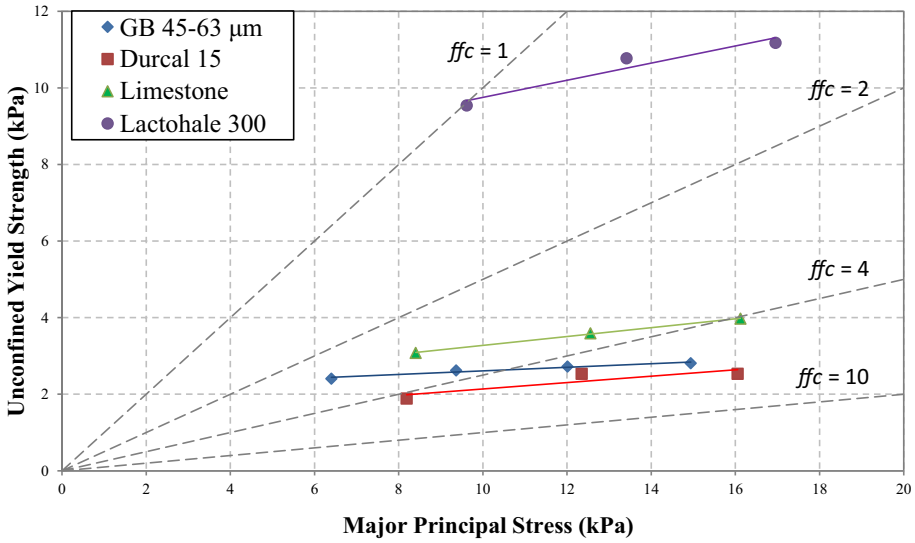

Fig. 3. Relationship between the major principal stress and unconfined yield strength at pre-shear normal stresses of 4, 6 and 8 kPa for the test materials. For glass ballotini an additional stress was also used.

Table 2
Flowability assessment of the powders tested at pre-shear normal stresses of 4–8 kPa based on Jenike [7] criteria.

Material	Flow function coefficient, *ffc*	Flow classification
Silanised glass ballotini 45–63 µm	2.7–4.4	Cohesive - easy flowing
Durcal 15	2.7–6.3	Cohesive - easy flowing
Lactohale 300	1.0–1.6	Very cohesive
BCR Limestone	2.7–4.1	Cohesive – easy flowing

indenter. The spherical indenter used in this study is a high precision glass bead supplied by Sigmund Lindner GmbH (Warmensteinach, Germany), having particle density of 1.53 kgm^{-3} and average roughness, R_a, of 0.08 µm. During the ball indentation test, the applied load, F, and the penetration of indenter, h, were continuously recorded throughout the process. The determination of hardness of the powder bed, representing the flow resistance, is based on the maximum indentation load, F_{max}, and projected area of the impression after the load is removed. The hardness of the powder bed, H, is calculated using Eq. (3).

$$H = \frac{F_{\max}}{A} \tag{3}$$

where A is the projected area of the impression of the indenter which is obtained using Eq. (4).

$$A = \pi h_c (d_i - h_c) \tag{4}$$

where d_i is the diameter of the indenter and h_c is the plastic depth, determined by the intercept of the tangent to the unloading curve [6,24]. The standard operating procedure and window for the Ball Indentation Method (BIM) established by Zafar et al. [24] were followed in this work.

The experimental setup for dynamic hardness measurement is different compared to the quasi-static method, as the approach is based on the impact of a ball on a compacted powder bed. It consists of a transparent tube of about 5 mm internal diameter which has vertical distance markings on the surface. A high precision spherical glass indenter is dropped from a predetermined height in order to accelerate the indenter under gravity to an appropriate velocity for impact on to the powder bed. A string with negligible weight is glued at the end of the glass indenter in order to retract it up the tube after the drop, to avoid damage to the indentation zone. Unlike indentation hardness, where the load is directly measured, dynamic indentation measures the hardness by a correlation proposed by Sundararajan and Shewmon [23] which is given by Eq. (5),

$$H_d = \frac{MV_i^2}{2U} \tag{5}$$

where M is the mass of the indenter, V_i is its incident velocity and U is the unrelaxed volume of the indentation impression. The mass of the indenter, M, is measured using a high precision digital scale, whilst the incident velocity, V_i, is determined using a high speed camera (Photron FASTCAM SA5) at 1000 frames per second. In order to calculate the unrelaxed volume, U, the depth of the penetration was determined from the images taken by the camera using the distance lines marked on the surface of the tube. The unrelaxed volume is given by Eq. (6), as illustrated by the schematic diagram of the powder bed after dynamic indentation in Fig. 4.

$$U = \frac{\pi h}{6}\left(3R_a^2 + h^2\right) \tag{6}$$

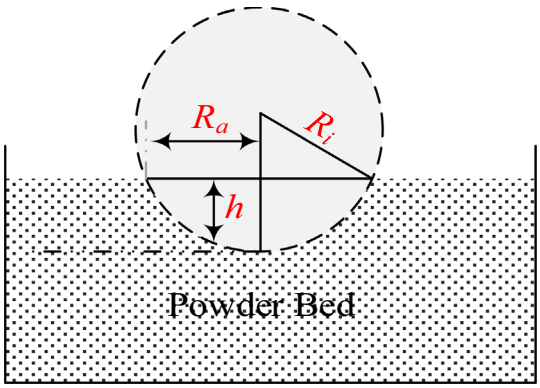

Fig. 4. Schematic diagram of ball indentation penetration into the powder bed.

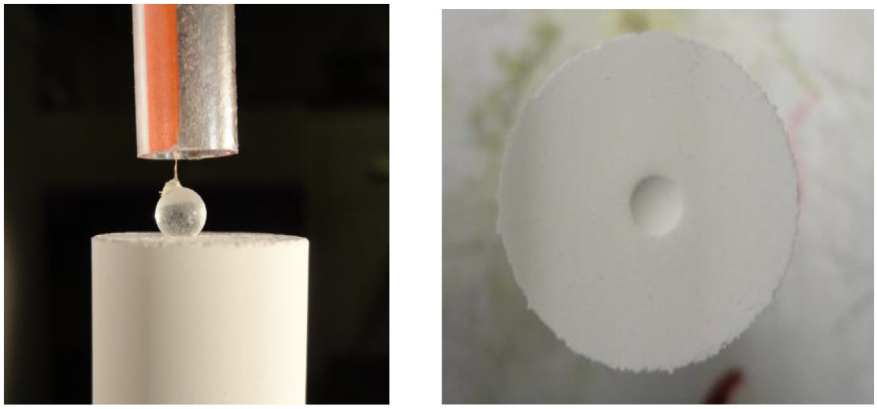

Fig. 5. Image of the ball indenter after the impact (left), and top view of the indentation impression after removing the indenter with the attached string (right).

According to the above schematic diagram, an expression for the height of the penetration (h) and the radius of the impression (R_a) can be determined using post image analysis. In this study, ImagePro software was used to analyse the side view of the indentation image (Fig. 5) to determine R_a and h.

3. Results and discussions

Initially experiments in the quasi-static regime were performed using three different penetration speeds (10 mm/min, 50 mm/min and 100 mm/min), the greatest of which represented the operational limit of the Instron machine. Indentation hardness measurements as a function of pre-consolidation normal stress were made for silanised glass ballotini, Durcal 15, Lactohale 300 and BCR limestone and the results are shown Fig. 6.

The result shows that the hardness, i.e. the flow resistance, increases with preconsolidation stress for the range tested (3–15 kPa) for all the powders tested. The hardness measurement for the Lactohale 300 sample is the highest amongst the samples. The hardness remains insensitive to the penetration speed, corresponding to different strain rates as the indenter size is fixed, with the increase from 10 to 100 mm/min for all four powders. The maximum dimensionless strain rate achieved was 0.015, which lies in the slow flow or quasi-static regime. Based on the boundaries defined by [21], the dimensionless strain rate required to the transfer from the quasi-static to the intermediate flow regime is approximately 0.15–0.25.

The dynamic indentation tests were carried out at pre-consolidation normal stresses of 5, 8, 10 and 15 kPa by dropping the ball from heights of 20, 50 and 160 mm, which gave the incident velocities of approximately 0.35, 0.75 and 1.50 m/s, respectively. This corresponds to strain rates of 50 to 330 s^{-1}, calculated by dividing the incident velocity by

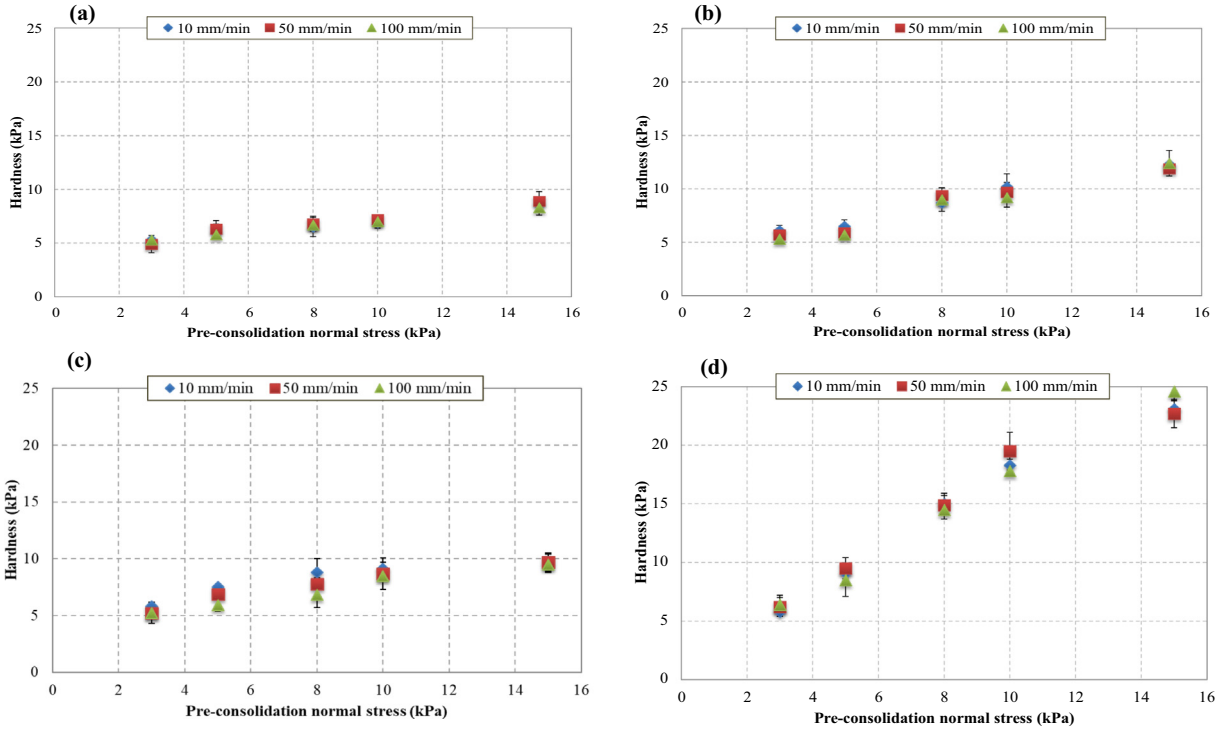

Fig. 6. Hardness measurement as a function of pre-consolidation normal stress at three different penetration speeds in the quasi-static regime for (a) silanised glass ballotini, (b) Durcal 15, (c) BCR limestone and (d) Lactohale 300.

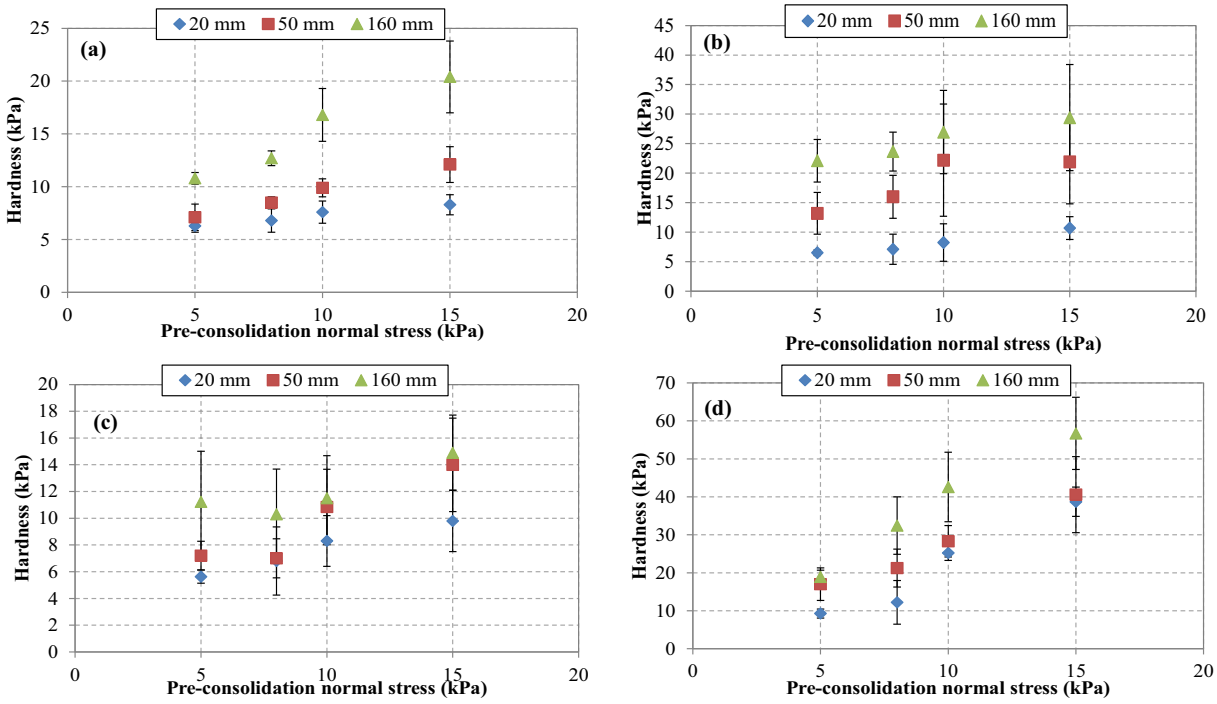

Fig. 7. Dynamic indentation hardness versus pre-consolidation stress for (a) silanised glass ballotini, (b) Durcal 15, (c) BCR limestone and (d) Lactohale 300 at different drop heights.

the maximum indentation depth (V_i/h). In all the cases, the penetration depth was smaller than the indenter radius and within the operational range defined by Zafar et al. [24]. The hardness as a function of pre-consolidation stress for the four samples tested is shown in Fig. 7.

It can be seen that the level of fluctuations in the hardness measurement (the error bars indicating one standard deviation of the fluctuations for three measurement repeats) increase with the height of fall of the indenter and also to a minor extent with the pre-consolidation normal stress. This is in line with the findings of Tardos et al. [21] and Pasha et al. [18] for the intermediate and dynamic regimes. It can also be observed that with an increase in impact velocity as a result of drop height, the hardness increases for all the four tested powders. The hardness measurements obtained by dynamic ball indentation, calculated by Eq. (5), are shown as a function of shear strain rate in Figs. 8 (a) and (b) for 8 kPa and 15 kPa pre-consolidation normal stresses, respectively. The lines in the figures just show the trends, which are remarkably consistent between the two pre-consolidation loads. Interestingly, BCR limestone does not show any sensitivity to strain rate and its flow resistance is low and almost independent of pre-consolidation stress in this range. The latter trend is also the case for the cohesive glass ballotini, but it does respond to a minor extent to increasing strain rate. In contrast, both Lactohale 300 and Durcal are sensitive to both strain rate and applied pre-consolidation stress. The underlying causes of differences in the behaviour of the test powders require further analyses, taking account of powder properties as well as the influence of air drag arising from rapid deformation. Such analyses are most suited for combined Discrete Element Method and Computational Fluid Dynamics with high fidelity particle shape modelling.

The dimensionless shear strain rate is calculated for both quasi-static and dynamic measurements according to Eq. (1) and the hardness values for all the materials tested in this study for 15 kPa pre-consolidation normal stress are shown in Fig. 9.

The flow resistance of Lactohale 300 is the largest across the whole shear strain rate range as it is the most cohesive. It can be seen that the hardness increases with the dimensionless shear rate in the intermediate flow region ($\gamma^* > 0.15$), as shown by Pasha et al. [18], and supported by the similar increase in shear stress with dimensionless strain

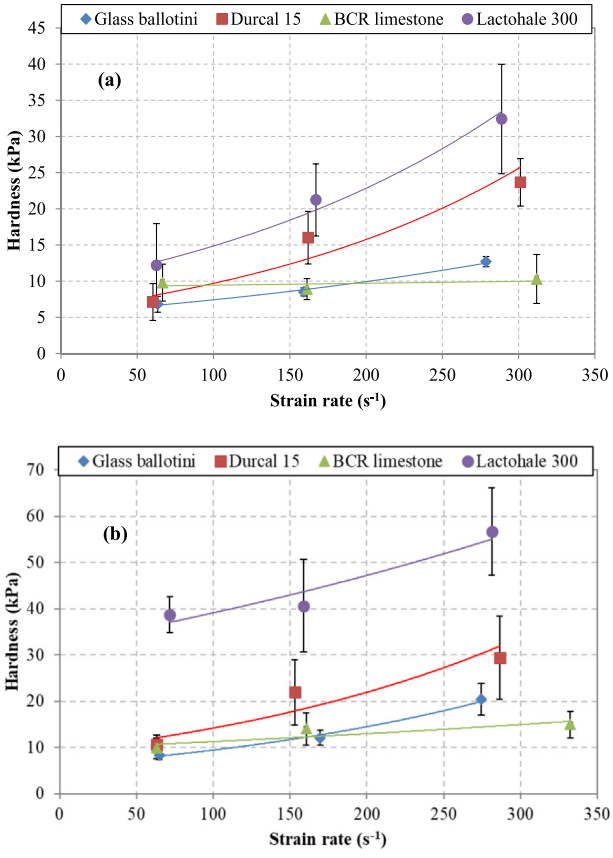

Fig. 8. Dynamic indentation hardness of the four test materials as a function of strain rate at (a) 8 kPa and (b) 15 kPa pre-consolidation normal stress.

rate observed by Tardos et al. [21] and (Vidyapati et al., 2012). This confirms that the flow resistance is dependent on the strain rate above a

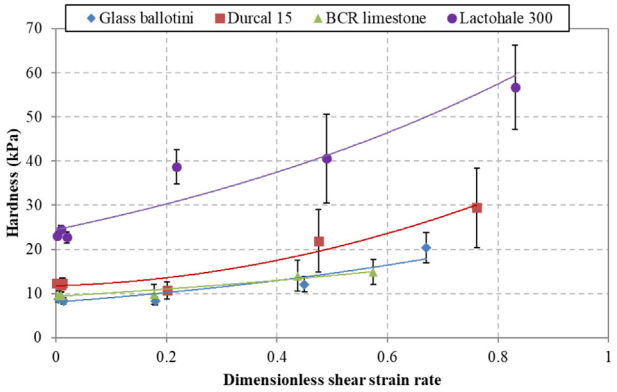

Fig. 9. Relationship between hardness and dimensionless shear strain rate for the four samples at 15 kPa pre-consolidation normal stress.

certain threshold. However, the trend depends on the material type. Lactohale 300 and Durcal 15 samples show a higher dependency compared to glass ballotini and limestone for the pre-consolidation stress of 15 kPa. This could be due to cohesion of the material, as Lactohale 300 is the most cohesive powder tested here, based on the flow function shown in Fig. 3. However, cohesion is not the only influencing factor as the particle shape, density and sliding friction are also different, so the link between these factors and strain rate dependency of flow resistance will require further investigation. It was also observed that as the dimensionless shear strain rate increased towards the rapid flow regime of 0.3, as identified by Tardos et al. [21], the dependency on strain rate becomes stronger. This is in line with the DEM simulations of Pasha et al. [18], who investigated the stress variations as a function of dimensionless strain rate in the dynamic ball indentation method by DEM. However, with the current experimental approach, only tests in the quasi-static and intermediate flow regimes could be carried out with maximum achieved incident velocity of 1.5 m/s (equivalent to dimensionless shear strain rate of approximately 0.85 for a 4.7 mm diameter indenter). In order to move from the intermediate to rapid flow regime, an incident velocity above 4 m/s is required for this indenter. The required drop height to reach a desired shear strain rate could be determined for any indenter and powder combination using the approach outlined by Tirapelle et al. [22]. However, this is beyond the scope of the current work, which was to explore the strain rate sensitivity of the ball indentation method, thus confirming that for instances where only a small powder quantity is available, this method could be usefully employed to establish the trend of the flow resistance with the shear strain rate.

4. Conclusions

In this study, dynamic hardness measurements were carried out on pre-consolidated powder beds of cohesive glass ballotini, Durcal 15, Lactohale 300 and BCR limestone at several indentation strain rates. It was shown that hardness measurement is independent of strain rate for the quasi-static regime, where the dimensionless shear strain rate, $\gamma^* < 0.15$. However, as the strain rate increases the flow resistance, represented by hardness, increases and the fluctuations in the measurements become more notable in line with the work reported in the literature. From the results presented in this study, the existence of a threshold boundary above which the hardness becomes dependent on the strain rate is evident. The information obtained corroborates well with the trends reported in the literature and shows that the ball indentation method can be used to assess powder flowability at high strain rates in instances where test materials quantity is limited.

Credit authors statement

Umair Zafar: Conceptualisation, Methodology, Analysis, Investigation, Writing-original draft. **Colin Hare:** Conceptualisation, Methodology, Review & Editing. **Ali Hassanpour:** Conceptualisation, Methodology, Review & Editing. **Mojtaba Ghadiri:** Conceptualisation, Methodology, Review & Editing, Supervision.

Declaration of Competing Interest

The authors declare that they have no known competing financial interests or personal relationships that could have appeared to influence the work reported in this paper.

Acknowledgements

The financial support of the Engineering and Physical Sciences Research Council, UK, through the Grant EP/G013047 is gratefully acknowledged.

References

[1] N. Berger, E. Azéma, J.-F. Douce, F. Radjai, Scaling behaviour of cohesive granular flows, EPL-Europhys. Lett. 112 (2015) 64004.
[2] S. Chiavlo, J. Sun, S. Sundaresan, Bridging the rheology of granular flows in three regimes, Phys. Rev. E 85 (2012) 021305.
[3] S. Dunatunga, K. Kamrin, Continuum modelling of projectile impact and penetration in dry granular media, J. Mech. Phys. Solids 100 (2017) 45–60.
[4] M. Ghadiri, M. Pasha, W. Nan, C. Hare, V. Vivacqua, U. Zafar, S. Nezamabadi, A. Lopez, M. Pasha, S. Nadimi, Cohesive powder flow: trends and challenges in characterisation and analysis, Kona Powd. Part. J. 37 (2020) 3–18.
[5] C. Hare, M. Ghadiri, Stress and strain rate analysis of the FT4 powder rheometer, EPJ Web Conf. 140 (2017) 03034.
[6] A. Hassanpour, M. Ghadiri, Characterisation of flowability of loosely compacted cohesive powders by indentation, Part. Part. Syst. Charact. 24 (2) (2007) 117–123.
[7] A.W. Jenike, Gravity Flow of Bulk Solids, Bulletin 108, Utah University, 1961.
[8] J.T. Jenkins, S.B. Savage, A theory for the rapid flow of identical, smooth, nearly elastic, spherical particles, J. Fluid Mech. 130 (1983) 187–202.
[9] J. Jenkins, D. Berzi, Dense, collisional, shearing flows of compliant spheres, EPJ Web Conf. 140 (2017) 01004.
[10] J.F. Klausner, D. Chen, R. Mei, Experimental investigation of cohesive powder rheology, Powder Technol. 112 (2000) 94–101.
[11] M. Krantz, H. Zhang, J. Zhu, Characterization of powder flow: static and dynamic testing, Powder Technol. 194 (3) (2009) 239–245.
[12] W.S. Lee, J.K. Chou, The effect of strain rate on the impact behaviour of Fe–2 mass on Ni sintered alloy, Mater. Trans. 46 (4) (2005) 805–811.
[13] C.K.K. Lun, S.B. Savage, J.T. Jenkins, N. Chepurniy, Kinetic theories for granular flow: inelastic particles in Couette flow and slightly inelastic particles in a general flow field, J. Fluid Mech. 140 (1984) 223–256.
[14] B.H.L. May, L. Golick, C.K. Phillips, M. Shearer, E.K. Daniels, Shear-driven size segregation of granular materials: Modelling and experiment, Phys. Rev. E 81 (5) (2010) 051301.
[15] G.D.R. MiDi, On dense granular flows, Eur. Phys. J. E 14 (2004) 341–365.
[16] P. Mort, J.N. Michaels, R.P. Behringer, C.S. Campbell, L. Kondic, M. Kheiripour Langroudi, M. Shattuck, J. Tang, G.I. Tardos, C. Wassgren, Dense granular flow – a collaborative study, Powder Technol. 284 (2015) 571–584.
[17] W. Nan, M. Ghadiri, Y. Wang, Analysis of powder rheometry of FT4: effect of air flow, Chem. Eng. Sci. 162 (2017) 141–151.
[18] M. Pasha, C. Hare, A. Hassanpour, M. Ghadiri, Numerical analysis of strain rate sensitivity in ball indentation on cohesive powder beds, Chem. Eng. Sci. 123 (2015) 92–98.
[19] S.B. Savage, D.J. Jeffrey, The stress tensor in a granular flow at high shear rates, J. Fluid Mech. 110 (1981) 255–272.
[20] S.B. Savage, M. Sayed, Stresses developed by dry cohesionless granular materials sheared in an annular shear cell, J. Fluid Mech. 142 (1984) 391–430.
[21] G.I. Tardos, S. McNamara, I. Talu, Slow and intermediate flow of a frictional bulk powder in the Couette geometry, Powder Technol. 131 (1) (2003) 23–39.
[22] M. Tirapelle, A.C. Santomaso, C. Hare, Dynamic ball indentation for powder flow characterization, Powder Technol. 360 (2020) 1047–1054.
[23] G. Sundararajan, P.G. Shewmon, The use of dynamic impact experiments in the determination of strain rate sensitivity of metalss and alloys, Acta Metall. 31 (1) (1983) 101–109.
[24] U. Zafar, C. Hare, A. Hassanpour, M. Ghadiri, Ball indentation on powder beds for assessing powder flowability: analysis of operation window, Powder Technol. 310 (2017) 300–306.